

Domains of apoE Required for Binding To apoE Receptor 2 and To Phospholipids: Implications For The Functions Of apoE in the Brain[†]

Xiaoping Li,[‡] Kyriakos Kypreos,^{‡,§} Eleni E. Zanni,[‡] and Vassilis Zannis*[‡]

Section of Molecular Genetics, Whitaker Cardiovascular Institute, Departments of Medicine & Biochemistry, Boston University School of Medicine, Boston, Massachusetts 02118

Received October 31, 2002; Revised Manuscript Received April 8, 2003

ABSTRACT: We have studied the contribution of the carboxy terminal domains of lipid-free apoE isolated from apoE-expressing cell cultures in binding to phospholipids and have determined the affinities of reconstituted POPC–apoE particles for the apoER2. It was found that the initial rate of association of apoE2, apoE3, apoE4, and a mutant form apoE4R158M to multilamellar DMPC vesicles was similar and was reduced and eventually diminished by gradual deletion of the carboxy terminal segments. The truncated apoE forms retained their ability to associate with plasma lipoproteins. Receptor binding studies were performed using the *ldlA*-7 cells expressing apoER2 and transiently transfected COS-M6 and the appropriate control untransfected cells. Specific binding to apoER2 was obtained by subtracting from the total binding to the receptor-expressing cells the nonspecific binding values of the untransfected cells. POPC–apoE particles generated using apoE3, apoE4, the truncated apoE4-259, apoE4-229, apoE4-202, and apoE-165, and the mutant apoE4R158M all bound tightly to the apoER2 (K_d range of 12 ± 3 to 19 ± 4 $\mu\text{g/mL}$). POPC–apoE2 bound with reduced affinity ($K_d = 31 \pm 5.3$ $\mu\text{g/mL}$). The findings establish that the apoER2 binding domain of apoE is in the 1–165 amino terminal region, whereas the carboxy terminal 230–299 region of apoE is required for efficient initial association with phospholipids.

Apolipoprotein E (apoE) is an important protein that is required for the homeostasis of cholesterol and other lipids in the circulation (1, 2). ApoE is the ligand for the LDL¹ receptor as well as other cell receptors (3–7). In vitro and in vivo studies have shown that mutations in apoE that prevent binding of apoE-containing lipoproteins to the LDL receptor are associated with high plasma cholesterol levels and cause premature atherosclerosis in humans and experimental animals (8–10). ApoE may also be involved in cholesterol efflux processes (11–14) and thus contribute to cell and tissue cholesterol homeostasis and protection from atherosclerosis (15, 16).

In addition to its role in either the pathogenesis of or protection from cardiovascular disease, apoE has also been implicated in Alzheimer's disease (17–19). ApoE is the only

apolipoprotein expressed locally in the brain (20, 21), and it is possible that it also plays an important role in lipid homeostatic mechanisms in the brain. In addition, biochemical and functional data suggest isoform specific functions of apoE, including differences in binding of apoE to A β (22–26), to tau and MAP2C (27), and to soluble APP (28). ApoE isoforms also affect differently the cholinergic deficit in the frontal cortex and the hippocampus (29, 30), the neuronal morphology and cytoskeletal structure in cell cultures (31, 32), the neuronal degeneration and dendritic remodeling in vivo (33), and the A β deposition and plaque-associated neuritic dystrophy in transgenic mice (34–36).

The interaction of apoE with lipids is crucial for the formation of lipoprotein particles, which are subsequently recognized and catabolized by several cell receptors (3–7). ApoER2, which is the subject of the current study, is a member of the LDL receptor family and has three different forms resulting from alternate splicing (6). ApoER2 binds only apoE-rich β -migrating VLDL with high affinity, as opposed to the LDL receptor, which binds both LDL and apoE-containing lipoproteins (6, 37). The difference in ligand specificity has been attributed to structural differences between the two receptors in the linker sequence, which connects with cysteine-rich repeats 4 and 5 (37). ApoER2 may also play an important role in brain development and functions mediated via its interaction with Reelin and activation of intracellular signaling pathways (38). ApoER2 is expressed in high levels in cortical and cerebellar layers adjacent to layers that express Reelin. In double deficient *VLDLR*^{−/−} and *apoER2*^{−/−} mice, the expression of the *disable 1* (*Dab1*) gene is upregulated. These mice have an

[†] This work was supported by grants from the National Institute of Health (HL68216 and AG-12717) and the Alzheimer's Association (IIRG-002220) to V.I.Z. and the EU Fifth Framework Program (MCIF No. 2000-02051) to K.E.K.

* To whom correspondence should be addressed.

[‡] Boston University School of Medicine.

[§] Present address: Department of Human and Clinical Genetics, Leiden University Medical Center, 2333 AL, Leiden, The Netherlands.

¹ Abbreviations: apoER2, apoE receptor 2; BCA, bicinchoninic acid; CETP, cholesteryl ester transfer protein; CHO, Chinese hamster ovary; DMEM, Dulbecco's modified Eagle's medium; DMPC, dipalmitoyl-phosphatidylcholine; FAF-BSA, fatty acid-free bovine serum albumin; HDL, high-density lipoprotein; apoE, apolipoprotein E.; ApoER2, apolipoprotein E receptor 2; LCAT, lecithin:cholesterol acyltransferase; LDL, low-density lipoprotein; *ldlA*, LDL receptor deficient CHO cell line; *ldlA*[apoER2] cells, apoER2-expressing *ldlA* cells; PMSF, phenylmethylsulfonyl fluoride; PAGE, polyacrylamide gel electrophoresis; POPC, 1-palmitoyl-2-oleoyl-L-phosphatidylcholine; rHDL, discoidal reconstituted HDL particles; SR-BI, scavenger receptor class B type I.

inversion of cortical layers and absence of cerebellar foliation and hyperphosphorylation of tau, which inhibits microtubule assembly (39). The phenotype of these mice resembles that of mice deficient in Reelin or Dab1 (39). These findings suggested binding of Reelin to apoER2, and the VLDL receptor activates intracellular signaling pathways that are initiated by phosphorylation of Dab1 (40). To gain insight into important functions of apoE that may be relevant both to cardiovascular disease and to Alzheimer's disease, we have developed an efficient apoE expression system based on recombinant adenoviruses, which allowed us to generate large quantities of the natural apoE isoforms and mutant or truncated apoE forms. Analysis of the lipid and receptor binding properties of different apoE forms established that the amino terminal 1–165 region of apoE suffices for binding of apoE to apoE receptor, whereas the carboxy terminal 260–299 region promotes efficient interaction of apoE with phospholipids, a process that may be essential for the generation of apoE-containing lipoproteins in the brain.

EXPERIMENTAL PROCEDURES

Materials

The Klenow fragment of DNA polymerase I, T4 ligase, polynucleotide kinase, and restriction enzymes were purchased from New England Biolabs. Calf intestinal alkaline phosphatase was purchased from Stratagene (La Jolla, CA), and Vent polymerase was purchased from Promega. Other materials for the polymerase chain reaction were obtained from Perkin-Elmer. The Sequenase sequencing kit was purchased from U.S. Biochemical Corp. The oligonucleotides were purchased from GIBCO-BRL. Bactotryptone and bacto yeast extract were obtained from VWR (Pittsburgh, PA). DMEM was provided by Life Technologies. Dextran sulfate and epoxy-activated Sepharose 6B were purchased from Pharmacia, and the column was purchased from BioRad; Iodo-Beads iodination reagent and the D-salt dextran plastic desalting columns were purchased from Pierce. The sodium ^{125}I was purchased from NEN. The BCA assay kit was purchased from Pierce. Other reagents (and sources) were as follows: FAF-BSA, cholesterol, sodium cholate, and POPC; aprotinin, benzamidine, leupeptin, and PMSF (Sigma Chemical Co., St. Louis, MO); dialysis tubing (Spectrum Medical Industries, Inc., Los Angeles, CA); Ham's F-12 medium, fetal bovine serum (FBS), and trypsin/EDTA (JRH Biosciences, Lenexa, KS); and penicillin/streptomycin, glutamine, and G418 sulfate (GIBCO BRL Life Technologies, Inc., Grand Island, NY). All other reagents were purchased from Sigma, Bio-Rad, or other standard commercial sources as previously described (41). The expression plasmid containing the full-length apoER2 cDNA designated (pcDL-SR α -apoER2) was a generous gift of Dr. Tokuo Yamamoto of Tohoju University of Japan. The plasmid contains the pBR322 origin of replication, ampicillin resistance, and polyA sequences. The apoER2 gene is cloned in front of the SR α promoter.

Methods

Plasmid and Recombinant Adenovirus Constructions. For generation of apoE gene mutations, we have constructed two

intermediate sets of plasmids I and II (Figure 1A). Plasmid I (pBlueEexIV) contains the EcoRI-EcoRI apoE gene region consisting of exon IV and part of the flanking introns cloned in pBluescript plasmid II KS $^+$ vector. This plasmid was constructed with the apoE2, apoE3, or apoE4 or mutated exon IV sequence (plasmid I). The following protocol was utilized for generation of additional mutations: (i) mutations were introduced in exon IV by polymerase chain reaction (PCR) amplification and mutagenesis using the pBlueEexIV derivatives (plasmid I) as a template and a set of two external primers spanning for instance the StyI-BbsI region and mutagenic primers covering the region that needs to be mutagenized. The primers used are shown in Table 1. The amplified mutant sequence is used to replace the corresponding pBlueEexIV sequence in the pBlueEexIV derivative (plasmid I).

The wild-type (WT) and mutant exon IV sequences were excised from the pBlueEexIV plasmid and cloned into the EcoRI site of the pGEM7-apoE-ExII,III vector to generate pGEM7-apoE4 (plasmid II). The parental vector pGEM7-apoE-ExII,III contains the 1507 bp MscI-EcoRI fragment of apoE genomic DNA (nucleotides 1853–3360), which includes exons II and III, cloned into the SmaI-EcoRI sites of pGEM7 vector. The correct orientation of the 1911 bp EcoRI insert in plasmid II was checked by restriction digest with NotI and XbaI and verified by DNA sequencing. The entire HindIII-XbaI fragment from pGEM7-apoE4 vector was excised with HindIII and XbaI digestion and cloned into the corresponding sites of the pAdTrack-CMV adenovirus shuttle plasmid to generate the different pAdTrack-CMV-apoE vectors (plasmid III). To generate the recombinant adenoviruses containing the WT and variant apoE forms, each of the pAdTrack-apoE vectors (plasmid III) was used to electroporate BJ 5183 *Escherichia coli* cells along with the pAd Easy-1 helper vector, which contains the viral genome and the long terminal repeats of the adenovirus (42). Recombinant bacterial clones resistant to kanamycin were selected and characterized. The recombinant virus vectors expressing WT apoE and mutant apoE forms were propagated in RecA DH5a cells and then linearized with PacI and used to infect 911 cells (43). Recombinant viruses were produced by large scale infection of 293 cells and purified by two successive CsCl ultracentrifugation steps. The virus produced was dialyzed extensively against 1X TD buffer (13.7 mM NaCl, 5 mM KCl, 0.73 mM Na₂HPO₄, 25 mM Tris, 0.9 mM CaCl₂, 0.5 mM MgCl₂), pH 7.8, and then stored at -80°C . Usually, titers of approximately 5×10^{10} pfu/mL were obtained.

Characterization of the Mutant ApoE Forms. The characterization of the apoE mutants was performed by one- or two-dimensional (2D) analysis of the secreted apoE, either following ^{35}S labeling or after purification as described (44).

Adenoviral Infection of Large-Scale Cultures of Infected HTB-13 Cells. For the large-scale production of apoE, HTB-13 cells were grown in roller bottles as described (45). The medium of the roller bottles was harvested after 24 h, filtered through a 0.4 μm filter, and stored at -80°C or run in the ion exchange column directly for purification. The harvest was repeated 4–7 times. Yields of 50–100 mg/L apoE were obtained.

Purification of Lipid-Free ApoE by Ion Exchange Chromatography Using Dextran Sulfate Sepharose Column. ApoE

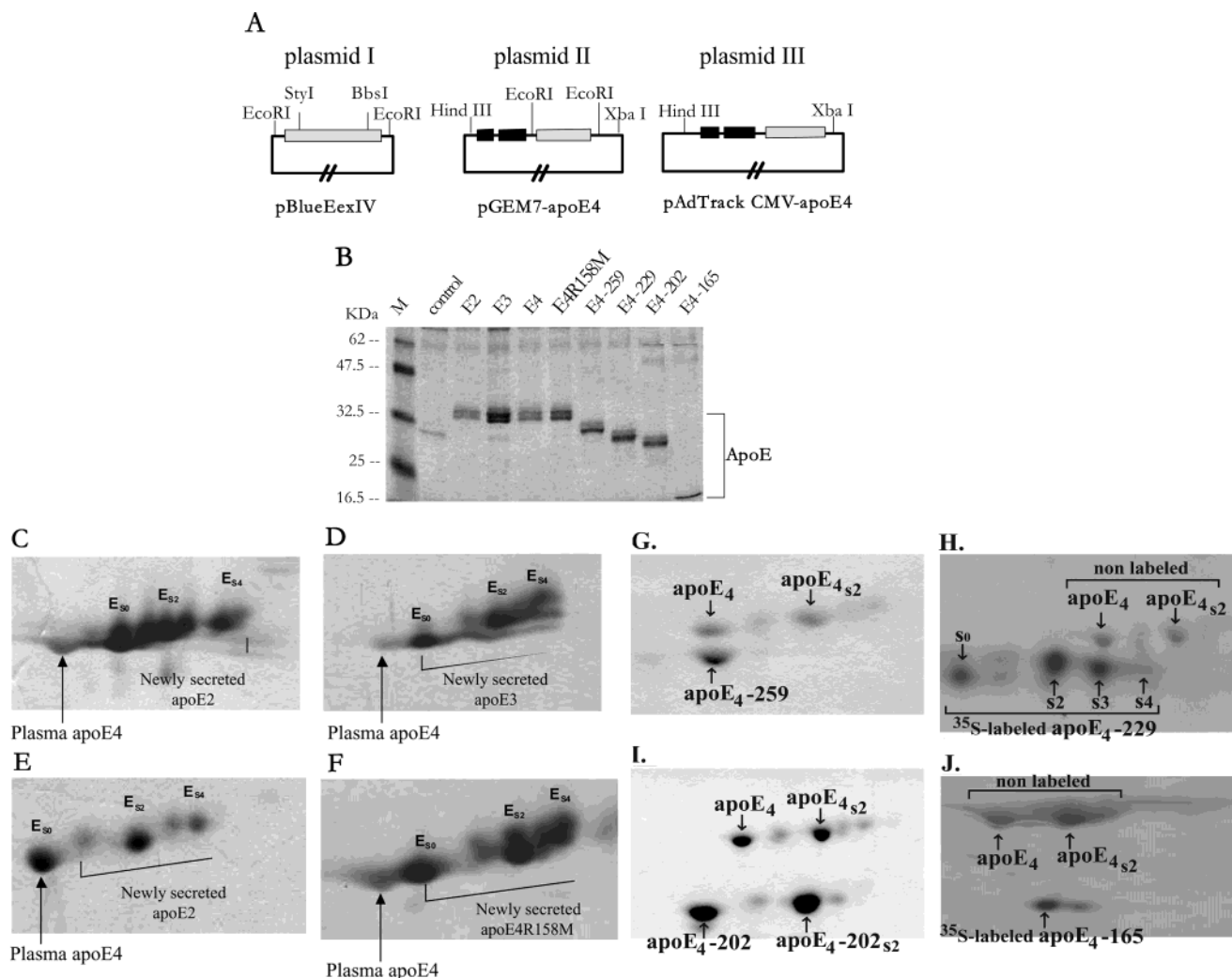


FIGURE 1: (A–J) Generation, characterization, and purification of WT and mutant apoE forms. (A) apoE gene plasmids used to generate the recombinant adenoviruses expressing the different apoE forms shown in the lower panel. (B) SDS–PAGE analysis of culture medium of HTB-13 cells infected with human apoE isoforms and variant apoE forms. Six microliters of culture medium was analyzed. M indicates protein MW markers of different M_r (New England Biolabs), indicated as follows: 32.5 kDa = rabbit muscle triosephosphate isomerase, 25 kDa = bovine milk β -lactoglobulin A, 16.5 kDa = chicken egg white lysozyme, and 47.5 kDa = rabbit muscle aldolase. (C–J) Comparison of the 2D patterns of apoE4 with that of full-length and truncated apoE forms. The charge and isoelectric point differences of the full length apoE forms and the apoE4R158M apoE4 and apoE4-185 mutant were established by 2D gel electrophoresis following ^{35}S labeling of the apoE-producing cell cultures. For this analysis, media obtained from ^{35}S -labeled cells transfected with constructs expressing the corresponding apoE forms were immunoprecipitated with antihuman apoE antibodies and analyzed by 2D PAGE and autoradiography using 5–10 μg of VLDL from a subject with apoE4/4 phenotype or 10 μg of purified apoE4 as an internal marker. The Coomassie brilliant blue-stained gel obtained from this analysis showed the position of the apoE4 that was included in the sample, and the autoradiogram showed the position of the newly synthesized apoE. Panels C–F, H, and J show superimposition of the autoradiogram on the gel that was stained with Coomassie brilliant blue. Panels G and I show 2D patterns of mixtures of unlabeled apoE4 with truncated apoE4 forms stained with Coomassie brilliant blue. The apoE used was purified from the culture media of cells following infection with recombinant adenovirus expressing the indicated apoE forms, as shown in Figure 2. These analyses established the charge and size differences between the apoE4 and the newly synthesized full-length and truncated apoE forms.

was purified from the culture medium of adenovirus-infected HTB-13 cells. The purification scheme involved dextran sulfate Sepharose column fractionation. Briefly, 30 mL of dextran sulfate Sepharose column was equilibrated with 20 mM Tris-HCl, 0.2 M NaCl, pH 7.4. A total of 2 L of apoE containing culture medium was concentrated to 75 mL in an Amicon concentrator using membrane with a cutting molecular mass of 10 kDa, and the NaCl concentration was adjusted to 0.2 M and loaded over the column at a flow rate of ~ 80 mL/h. The column was eluted with a 120 mL 0.2–1.0 M NaCl gradient in 20 mM Tris-HCl, pH 7.4, at the same flow rate, and fractions of 3 mL were collected. The pure protein fractions were pooled and were dialyzed

extensively against 0.05 M NH_4HCO_3 and lyophilized. The protein yield was in the range of 20–30 mg/L depending on the apoE variant.

Binding of ApoE to Multilamellar Dimyristoylphosphatidylcholine (DMPC) Vesicles. To study the lipid binding properties of the WT and the various mutant forms of apoE, kinetic–turbidimetric methods as described by Pownall et al. (46) were used. DMPC dissolved in a glass-distilled chloroform:methanol (2:1) solution was placed in a glass tube. The sample was dried under nitrogen, and the appropriate amount of a 5 mg/mL solution of apoE in a 10 mM Tris-HCl, pH 8, 150 mM NaCl, 1 mM NaN_3 , and 0.01% EDTA buffer was added to it, to give a final DMPC:apoE ratio of

Table 1: Oligonucleotides Used for Mutagenesis and Mutants Created^a

oligonucleotide name	oligonucleotides	mutations	designation of mutants
outside primer S	5' CAG GCC CGG CTG GGC GCG G 3'		
outside primer A	5' G GGG TCG CAT GGC TGC AGG C 3'		
E260RXS	5' ATT CCA GGC CTG ACT CAA GAG CTG 3'	apoE4 Arg (CGC) 260→stop (TGA)	apoE4-259
E260RXA	5' CAG CTC TTG AGT CAG GCC TGG AAT 3'		
E230DXS	5' GAC CGC CTG TAG GAG GTG AAG GAG 3'	apoE4 Asp (GAC) 230→stop (TGA)	apoE4-229
E230DXA	5' CCT TCA CCT CCT ACA GGC GGT CGC 3'		
E3203LXS	5' GGC CAG CCG TGA CAG GAG CGG GCC 3'	apoE4 Leu (CTA) 203- -stop (TGA)	apoE4-202
E3203LXA	5' CCG CTC CTG TCA CGG CTG GCC GGC 3'		
E3166AXS	5' CAG GCC GGG TGA CGC GAG GGC 3'	apoE4 Ala (GCC) 166→stop (TGA)	apoE4-165
E3166AXA	5' GCC CTC GCG TCA CCC GGC CTG 3'		
E 158 M-S	5' C CTG CAG AAG ATG CTG GCA GTG TAC 3'	apoE4 Arg (CGC) 158→Met (ATG)	apoE4R158M
E 158 M-A	5' GTA CAC TGC CAG CAT CTT CTG CAG G 3'		

^a Bold characters represent the mutated codons.

2.5:1 (W/W), with protein at a final concentration of 0.2 mg/mL. The experiment was performed at 24 °C, and the absorbance at 325 nm was monitored at 5 min intervals for 90 min using a Perkin-Elmer Lambda 3A spectrophotometer.

Preparation of rHDL Containing ApoE (POPC–ApoE). POPC was used to prepare the reconstituted discoidal POPC–apoE particles employing the sodium cholate dialysis method with only minor modifications (47). POPC–apoE particles were prepared from a molar ratio of 100:10:1:100 of POPC:cholesterol:apoE:Na cholate. In a typical experiment, 0.14 mg of cholesterol and 2.71 mg of POPC were placed in glass tubes, vortexed gently, and dried under nitrogen. The dried lipid was dissolved in a 10 mM Tris-HCl, pH 8, 150 mM NaCl, 1 mM NaN₃, and 0.01% EDTA buffer by vortexing for approximately 30 s, followed by storage on ice. The process was repeated until the phospholipid was completely suspended in the buffer. This required approximately 2 h. The sodium cholate was added, and the solution was placed on ice for one more hour. Finally, the apoE (usually 1 mg) was added and the incubation on ice continued for another hour. To remove the sodium cholate, the solution was dialyzed against 5–6 L of the 10 mM Tris-HCl, pH 8, 150 mM NaCl, 1 mM NaN₃, and 0.01% EDTA buffer at 4 °C, using tubing with a molecular mass cut off of 12–14 kDa. Finally, a gradient gel (8–25%) was run under native conditions at 15 °C on a Pharmacia Phast-gel system to ascertain the size of the particle or used for electron microscopy (EM) analysis described below. The POPC particles were stored at 4 °C under nitrogen to prevent the oxidation of lipids.

EM. POPC–apoE particles prepared with various mutant apoE forms as described above were analyzed by EM. To prepare the sample for EM, 50 µg of POPC–apoE was desalted three times using Amicon centrifugal filter devices (Microcon). The final concentration was approximately 1 mg/mL in deionized water. A 5 µL aliquot suspension of sample was applied for 10 s to a Formvar carbon-coated 300 mesh copper grid. The carbon film surface was made hydrophilic by glow discharge in a Balzers Union CTA 010 Glow Discharge apparatus and used immediately. Excess POPC–apoE suspension was removed by blotting with filter paper and immediately replaced with a 5 µL droplet of 1% sodium phosphotungstate, pH 7.4. After a few seconds, excess stain was removed and the grid was air-dried. Fields of particles were photographed with a Philips CM12 electron microscope (Philips Electron Optics, Eindhoven, The Netherlands).

Iodination of ApoE. ApoE was labeled by ¹²⁵I using Iodo-Beads (48) iodination reagent and Na ¹²⁵I (New England Nuclear). Each reaction used 1 mCi ¹²⁵I and three beads and 1 mg of apoE. The reaction was carried out in Tris-HCl buffer (10 mM Tris-HCl, pH 8, 150 mM NaCl, and 0.01% EDTA). An aliquot of 100 µL of Tris-HCl buffer was added to the ¹²⁵I container and mixed. The diluted radioactive ¹²⁵I solution was transferred to an Eppendorf tube containing 1–2 mg of apoE in the form of POPC–apoE particles in Tris-HCl salt buffer. The final volume was adjusted to 900 µL using Tris-HCl salt buffer. The sample was placed in a lead pig. Just prior to use, beads were washed with 500 µL of Tris-HCl salt buffer per bead and dried on a filter paper (this washing step removed any loose particles and reagent from the beads). The beads were added to the reaction solution and kept at room temperature for 45 min with mixing every 5–10 min. The reaction was terminated by removing the solution from the reaction vessel. The ¹²⁵I-labeled apoE was separated from the unincorporated Na¹²⁵I by gel filtration using Pierce's Presto Desalting Columns (Pierce, Inc.). Ten fractions (0.5 mL each) were collected, and 1 µL of each fraction was used for determination of the ¹²⁵I counts. Ten microliters of each fraction was used to measure the protein concentration by BCA protein assay (49). Another 10 µL of each fraction was used for PAGE gel analysis of the sample. The specific activity was calculated based on the protein concentration and the ¹²⁵I counts and expressed as cpm/µg of protein. Specific activities of 1000–1500 cpm/ng protein were obtained.

Receptor Binding Assay. IdIA-7 is an LDL receptor deficient CHO cell mutant (50, 51). The IdIA[apoER2] cells, a generous gift of Dr. Tokuo Yamamoto of Tohoku University of Japan, are IdIA-7 cells stably transfected with the expression plasmid pcDL-SRα apoER2, described above. Both cell lines were maintained in monolayer culture in Ham's F12 medium containing 5% FBS, 100 units/mL penicillin, 100 units/mL streptomycin, and 2 mM glutamine. All incubations with cells were performed at 4 °C in a humidified 5% CO₂, 95% air incubator.

ApoER2 binding at 4 °C was assessed by measuring cell association of radiolabeled ligands. Briefly, on day 0, cells (both IdIA-7 and IdIA[apoER2]) were plated at concentrations of (4.5–5) × 10⁴ cells/well in 24 well dishes in complete F12 medium. On day 2, the monolayers were washed twice with Ham's F12 medium and then refed with 0.4–0.5 mL of medium (Ham's F-12 containing 0.5% (w/v) FAF-BSA, 100 units/mL penicillin, 100 units/mL streptomycin, 2 mM

glutamine) with the indicated radiolabeled ligands [125 I] (POPC–apoE). Eight different concentrations, ranging from 0.5 to 100 μ g/mL, were used, and the experiments were performed in duplicate. After a 1.5 h incubation at 4 °C, the cells were washed twice at 4 °C with buffer B (50 mM Tris-HCl, pH 7.4, 0.15 M NaCl) containing 2 mg/mL FAF-BSA, followed by one rapid wash with buffer B alone. The cells were then solubilized with 0.1 N NaOH (300 μ L each well). Aliquots of 200 μ L were used for radioactivity determinations, and 25 μ L was used for determination of the protein concentration using the BCA assay.

For receptor binding using transiently transfected cells, COS-M6 cells were grown in DMEM with 50 units/mL penicillin, 50 μ g/mL streptomycin, and 2 mM glutamine (medium A) supplemented with 10% FBS (medium B) at 37 °C in a humidified 5% CO₂, 95% air incubator with a control plasmid that did not encode a protein (pcDNA-1). COS-M6 cells (1.5×10^6) were plated in 100 mm dishes in medium B on day 0. On day 1, cells were transfected with the apoER2 expression vector (pcDL-SR α -apoER2) using the DEAE–dextran method as described previously (52). For apoE binding, cells were harvested with trypsin and replated in medium B containing [125 I] POPC 1 mM sodium *n*-butyrate on day 2 in 24 well dishes at 150 000 cells/well in 1 mL of medium B containing 1 mM sodium *n*-butyrate. Cells were used for receptor binding on day 3 as described above. The specific binding was obtained by subtracting the binding of the untransfected control cells (IdLA-7) from the binding of the receptor-expressing cell lines IdLA[apoER2] or the COS-M6 cells transiently transfected with the apoER2. Binding parameters K_d and B_{max} were determined on the basis of the specific binding curve using the Prism program (GraphPad Software, Inc.). The specific binding (cell association) values of the saturation curves are expressed as nanograms of apoE in the complex associated with the cells per mg of total cell protein.

RESULTS

Characterization of WT and Variant ApoE Forms Secreted by HTB-13 Cells Following Adenoviral Infection. One-dimensional sodium dodecyl sulfate (SDS)–PAGE performed for the truncated apoE forms established that apoE4-259, apoE4-229, apoE4-202, and apoE4-165 are smaller in size (apoE4-259, 28.5 kDa; apoE4-229, 25.2 kDa; apoE4-202, 22.2 kDa; and apoE4-165, 18.2 kDa as compared to an apparent M_r of 38 kDa for the full-length apoE. With the exception of apoE4-165, all of the other apoE forms contain several bands. Previous studies have established that the slower migrating forms are sialylated at residue 194 of apoE (53, 54) (Figure 1B). The charge and isoelectric point differences of the full-length apoE isoforms the mutant apoE4R158M and the truncated apoE forms were established by 2D gel electrophoresis following 35 S labeling of the apoE-producing cell cultures, as described previously (44).

It was found (Figure 1C–J) that as compared to the plasma apoE4, this newly synthesized apoE2, apoE3, and the apoE4R158M have 2, 1, and 1 more negative charges, respectively. Plasma apoE4 and the newly synthesized apoE4 overlap on the 2D gels. The E4-259, E4-229, E4-202, and E4-165 differ by 0, +3, +0.1, and –1 negative charges, respectively, as compared to the plasma apoE4. These charge

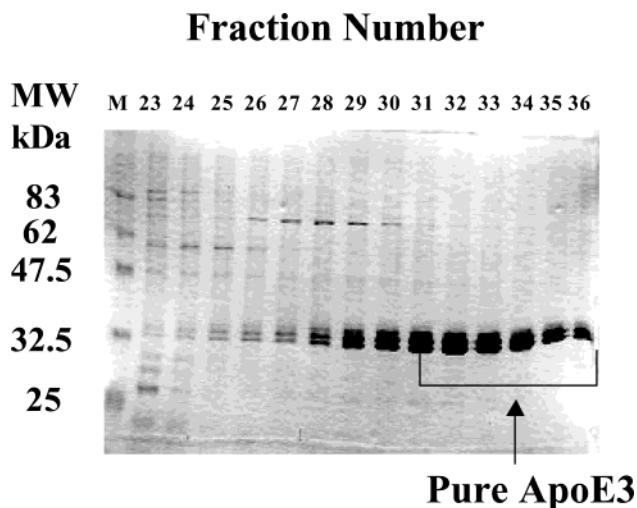


FIGURE 2: Purification of apoE4 from the culture medium of cells expressing apoE4. M indicates the position of protein markers of known M_r as indicated. Numbers correspond to fraction number.

differences are expected, based on the positive and negative residues lost in each of the truncated apoE forms.

Purification of ApoE from the Culture Medium of HTB-13 Cells Following Adenovirus Infection. HTB-13 cells lines expressing the different apoE forms were grown in large scale in roller bottles and infected with recombinant adenovirus as explained in the Experimental Procedures (45), and serum-free culture medium was collected. ApoE was purified from the culture medium by ion exchange chromatography using dextran sulfate Sepharose columns. Following loading and washing with 20 mM Tris buffer containing 0.2 M NaCl, the apoE was eluted by a 0.2–1 M NaCl gradient in the same buffer. Impurities are eluted in fractions 0–20, and pure apoE is eluted in fractions 31–36. A typical elution profile of apoE following SDS–PAGE is shown in Figure 2.

Generation and EM Analysis of Reconstituted POPC–ApoE Particles. The mutant proteins were reconstituted in particles containing POPC and cholesterol as described in the Experimental Procedures (47). The POPC–apoE particles were negatively stained with potassium phosphotungstate, overlaid on carbon-coated grids, and photographed with a Philips CM12 electron microscope. As shown in Figure 3A–H, the sodium cholate dialysis method allowed the formation of discoidal particles with all of the WT and the mutant apoE forms tested. Under the negative staining conditions used, these particles form the typical “rouleaux”, indicating that they are discoidal in shape and that they have the thickness of a phospholipid bilayer. To further characterize the size of the discoidal apoE/PC/C–apoE, cross-linking experiments were performed with particles isolated by gel filtration using sodium suberimidate. This analysis showed the presence of two apoE2 or apoE2-202 molecules per particle. The average size of POPC particles, determined from the EM pictures, was 174 ± 49 (data not shown).

Phospholipid Binding Properties of ApoE Isoforms and the Variant ApoE Forms. The lipid environment has profound effects on apoE conformation. DMPC binding experiments were performed to assess the effect of the mutations on the kinetics of interaction of apoE with multilamellar DMPC vesicles. The rate of the interaction was monitored by the

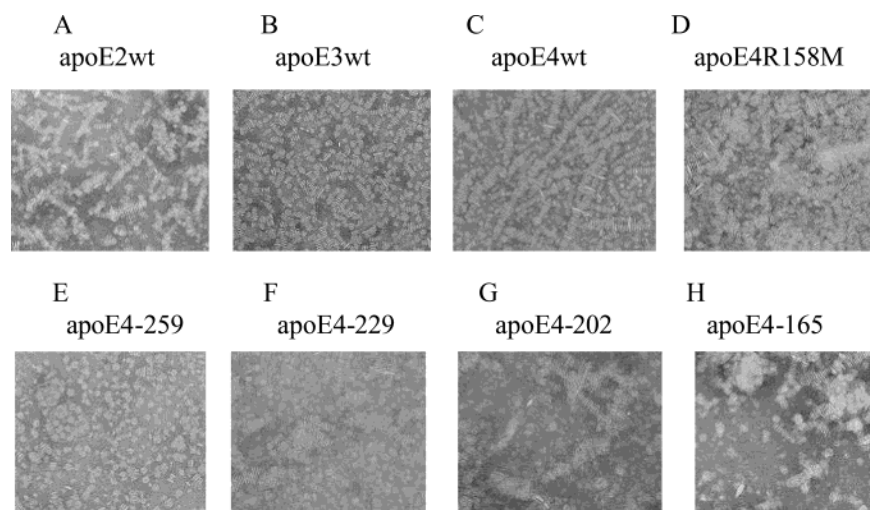


FIGURE 3: (A–H) EM of the discoidal POPC–apoE particles used as ligands for binding the apoER2. (A) apoE2, (B) apoE3, (C) apoE4, (D) apoE4R158M, (E) apoE-259, (F) apoE4-229, (G) apoE4-202, and (H) apoE-165.

change in absorbance at 325 nm. The experiments were performed at 24 °C, the transition temperature of the lipid, where the gel and liquid–crystalline phases coexist and where defects in the lipid matrix make it easier for apoE to interact.

It was found that all of the WT apoE2, apoE3, and apoE4 can solubilize multilamellar DMPC vesicles rapidly, as indicated by the decrease in turbidity of the DMPC dispersions as a function of time. We observed a small but reproducible increase in the rate of initial solubilization of the multilamellar DMPC vesicles by apoE4 as compared to apoE2, apoE3, and apoE4R158M (Figure 4A). A much greater difference exists in the rate of solubilization between apoE4 and plasma apoA-I (Figure 4A). In contrast, deletion of the carboxy terminal residues 260–299 of apoE reduces greatly the initial rate of solubilization of the multilamellar DMPC vesicles whereas deletion of residues beyond amino acid 229 results in a very slow rate of solubilization of the multilamellar DMPC vesicles by any of the three apoE mutants, apoE4-229, apoE4-202, and apoE4-165 (Figure 4B). These findings indicate that the carboxy terminal helices of apoE between residues 229 and 299 are critical for efficient interaction of apoE with phospholipids.

High Affinity Binding of Discoidal Reconstituted POPC–ApoE Particles to ApoER2. Previously studies have shown that apoE-enriched β VLDL binds to apoER2 (6). In the current study, we have focused on the binding specificity of apoE in the form of reconstituted POPC–apoE particles to apoER2. These apoE–apoER2 interactions may be significant for cholesterol homeostasis in the brain (6, 20) and may also influence A β polymerization (23–26) and receptor-mediated signaling (38). It is known that different cells contain several apoE-recognizing receptors (3–5, 7). To establish specific binding of POPC–apoE to apoER2, it was necessary to subtract the background binding of apoE to all of these receptors. For this purpose, binding studies were performed in IdIA-7 cells expressing apoER2[IdIA apoER2] cells and untransfected IdIA-7 cells. The specific binding curve and the binding parameters K_d and B_{max} were then determined by subtracting the binding values to the IdIA cell for every experimental point from the corresponding binding values to IdIA[apoER2] cells (Figure 5A). To ensure that

the specific values were valid and reflected the overexpression of apoER2 in the permanent cell line and not a fortuitous increase in expression of the endogenous apoER2, we performed receptor binding studies in the untransfected and the transiently transfected COS-M6 cells. The K_d obtained for IdIA[apoER2] permanent cell lines and the COS-M6 cells transiently transfected with an expression plasmid for apoER2 were similar (16 μ g protein/mL), whereas the total and specific binding were higher in the permanent cell line expressing apoER2 (Figure 5B).

Natural ApoE Isoforms and Mutant ApoE Forms Have Similar Affinities for ApoER2. Receptor Binding Is Maintained When the Carboxy Terminal Residues 166–299 Are Deleted. To address the question of whether specific domains or residues of apoE are involved in receptor binding, we have compared the binding of the natural apoE isoforms, one apoE mutant (apoE4R158M), and several truncated apoE forms extending to residues 259, 229, 202, and 165. The purpose of the mutations was to assess the importance of the carboxy terminal region of apoE as well as the participation of residue 158 of apoE to the apoER2 specific binding. It has been shown that residue R158 and the carboxy terminal region of apoE are important for binding of apoE containing lipoproteins to the LDL receptor (55–57). Our analysis showed that the apoE2, apoE3, the point mutant (apoE4R158M), and the truncated apoE forms bind to the apoER2 with similar affinities K_d in the range of 13–19 μ g/protein/mL (Figure 6A–H), suggesting that the amino terminal region 1–165 of apoE contains the determinant region for binding to apoER2. The affinity of apoE2 for apoER2 is reduced 25–50% as compared to the other apoE forms, $K_d = 31 \pm 5.3$ (Figure 6A and Table 2).

DISCUSSION

Background. Studies in humans and experimental animals have shown that apoE is required for the clearance of apoE containing lipoprotein remnants by the liver, a process that involves the LDL receptor and possibly heparan sulfate proteoglycans (58–61). Mutations in apoE that prevent binding to the LDL receptor are associated with type III hyperlipoproteinemia and premature atherosclerosis (1, 2, 8–10).

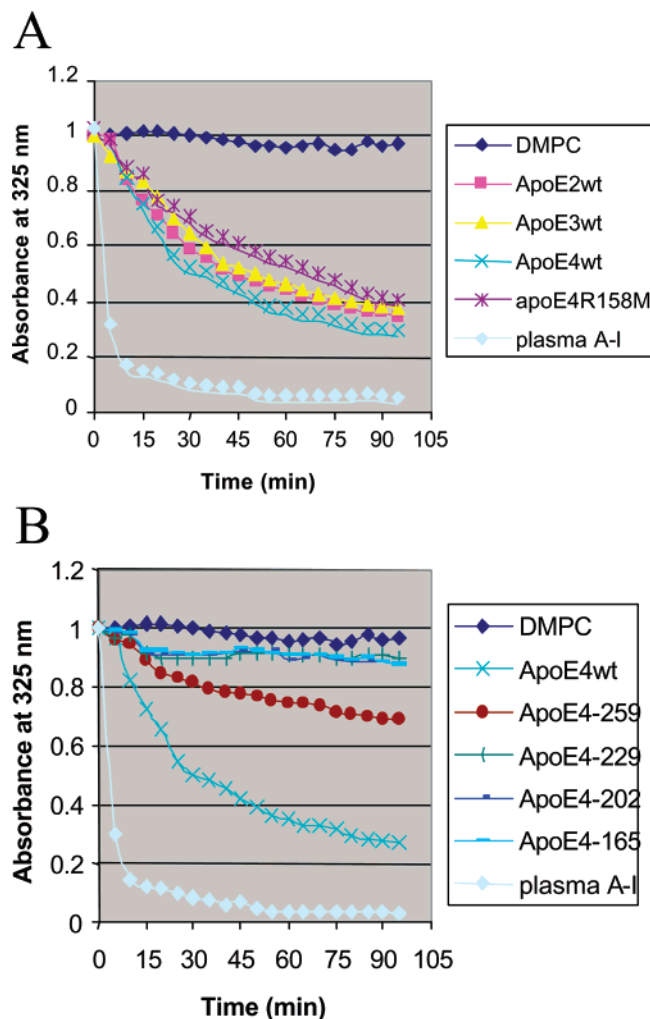


FIGURE 4: (A,B) Solubilization of multilamellar vesicles of DMPC by WT and mutated apoE forms monitored by the turbidity change as a function of time at 24 °C. Multilamellar vesicles of DMPC were combined with WT or variant apoE forms at a ratio of DMPC: apoE of 2.5/1 (w/w). The change in turbidity was monitored by the change in absorbance at 235 nm at 5 min intervals and was plotted as a function of time. ApoE forms utilized are indicated in the figure. (A) apoE2 wt, apoE3 wt, apoE4 wt, apoE4R158M, plasma apoA-I; (B) apoE2-259, apoE2-229; E2-202, apoE2-165.

In addition to its functions in lipid homeostasis in the circulation, apoE is the only apolipoprotein of the brain, where it is synthesized abundantly in astrocytes and glial cells (20, 21) and is found in lipoproteins of the cerebrospinal fluid (62). An obvious question that arises is what might be the physiological functions of apoE in the brain. A hint to this question was provided in the early 1990s when it was shown that one of the apoE isoforms, the apoE4, is a risk factor for Alzheimer's disease (AD) (18, 19). However, despite this important observation, our knowledge on the biogenesis and the functions of apoE-containing lipoproteins in the brain remains limited. To account for the association of apoE with AD, various hypotheses have been proposed, including lipid homeostatic mechanisms and cell signaling pathways involving apoE and apoE receptors (38–40). Because one of the apoE-recognizing receptors that is expressed abundantly in the brain is the apoER2 (6), the current study focused mainly on the interactions of apoE with the apoER2. These apoE/apoER2 interactions may be important for the catabolism of apoE-containing lipoproteins.

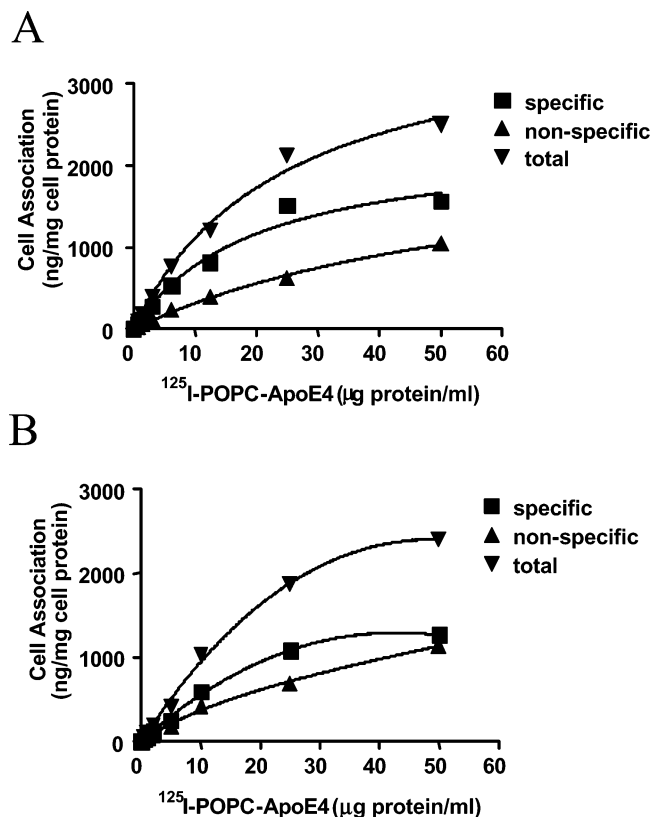


FIGURE 5: (A,B) Concentration-dependent binding of ¹²⁵I-apoE4–POPC complexes to confluent monolayers of IdIA CHO cells expressing apoER2 and control IdIA CHO cells. IdIA-7 cells and IdIA[apoER2] CHO cells in the microtiter wells were washed and incubated with various concentrations of ¹²⁵I-apoE–POPC. Total binding to the permanent IdIA[apoER2] cells and total binding to the COS-M6 cells transiently transfected with apoER2 and to the untransfected IdIA-7 and COS-M6 cells were obtained experimentally. The specific binding was determined by subtracting the binding curve of the IdIA-7 cells from the corresponding curve of the permanent cell line expressing the apoER2 (A) and the binding curves of the untransfected COS-M6 cells from the curve of the COS-M6 cells transiently transfected with the apoER2 (B).

In addition, the study examined the interaction of apoE with phospholipids and preexisting lipoproteins. These interactions may also be important for the biogenesis of apoE-containing lipoproteins.

Specific Binding of Reconstituted POPC–ApoE Particles to ApoER2. Brain cells contain numerous apoE-recognizing receptors (4, 5, 63–65), including the LDL receptor (64), the LRP (5), the VLDL receptor (65), and the apoER2 (6). Previous studies have shown that cell lines overexpressing apoER2 bind with high affinity and internalize apoE-enriched rabbit βVLDL (6). Several domains of apoE have been described, which are involved in LDL receptor binding (55, 57, 66, 67), heparin binding (68), and lipid and lipoprotein binding (69–72). The LDL receptor binding domain is found between residues 136–152 while neighboring residues may also indirectly affect receptor binding (55–57, 66, 67). Although the mode of binding of apoE-containing lipoproteins to the LDL receptor has been well-characterized, little is known on the interactions of human apoE containing lipoproteins with the apoER2.

It is known that different cells express various levels of apoE-recognizing receptors. To establish specific binding of apoE-containing lipoprotein particles to the human apoER2

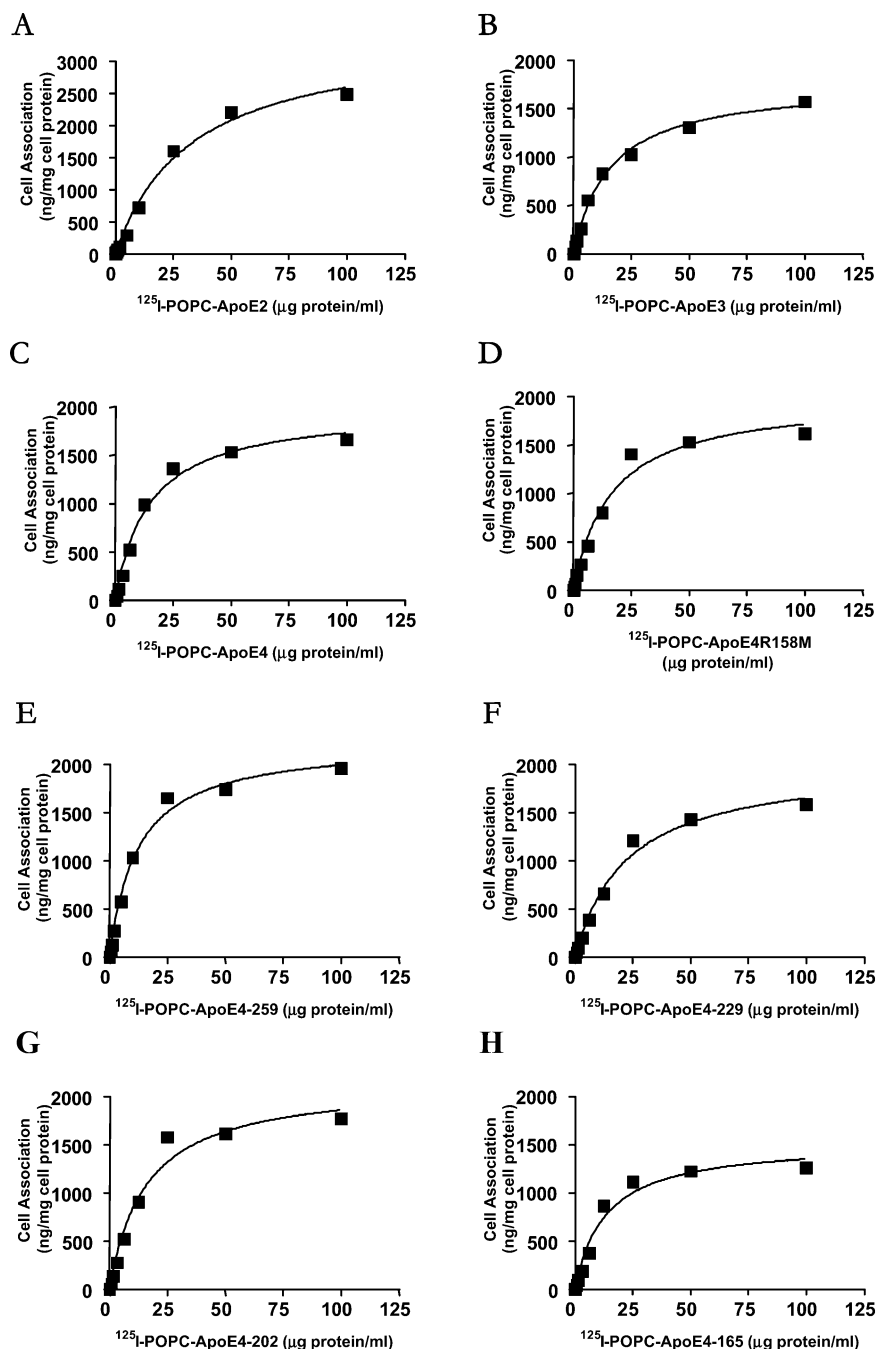


FIGURE 6: (A–H) Concentration-dependent binding of ^{125}I -apoE–POPC complexes containing different apoE isoforms and mutant and truncated apoE forms to confluent monolayers of LdlA-7 cells expressing apoER2. Cells in the microtiter wells were washed and incubated with various concentrations of ^{125}I -apoE–POPC (specific activity). Total binding to LdlA[apoER2] CHO cells and total binding to untransfected LdlA-7 cells were obtained experimentally. The specific binding shown in this figure was determined by subtracting the values of binding to the LdlA-7 cells from the corresponding values of binding to the LdlA[apoER2] cells. The specific activity of iodinated apoE was in the range of 1000–1500 cpm/ng. Two to four independent experiments were performed in duplicate for each apoE form. The average K_d and B_{\max} values thus determined are shown in Table 2. The apoE forms used are (A) apoE2, (B) apoE3, (C) apoE4, (D) apoE4158M, (E) apoE4-259, (F) apoE4-229, (G) apoE4-202, and (H) apoE4-165.

expressed by a permanent cell line (designated LdlA apoER2), it was necessary to subtract the background binding of apoE to all of the apoE-recognizing receptors present in the parent cell line that was designated LdlA. These experiments using the apoE4 isoform as a ligand established specific binding of POPC–apoE particles to the apoER2, which occurs with $K_d = 16 \mu\text{g/mL}$ and $B_{\max} = 2020 \text{ ng/mg cell protein}$.

To ensure that the specific binding values that we measured were valid, we also determined the apoER2-dependent binding following transient transfection of COS-

M6 cells with an apoER2-expressing plasmid. In this case, the binding to the untransfected COS-M6 cells was subtracted from the binding to the transfected cells. The K_d obtained using the transiently transfected COS-M6 cells was similar to that obtained using the permanent cell line LdlA[apoER2] ($K_d = 16 \mu\text{g/mL}$), whereas the total and specific binding were lower.

Effects of ApoE2 Mutations on the Binding of POPC–ApoE Particles to ApoER2. In the current study, we also examined the binding of three naturally occurring apoE forms

Table 2: Dissociation Constants (K_d) and B_{\max} of apoE–apoER2 Complexes Involving Different apoE Forms

apoE variant	<i>n</i>	K_d ($\mu\text{g protein/mL}$)	B_{\max} (ng/mg cell protein)
apoE2	5	31 ± 5.3	2978 ± 482
apoE3	5	13 ± 3.7	1943 ± 253
apoE4	5	16 ± 2.3	2020 ± 189
apoE4R158M	5	18 ± 4.0	2002 ± 215
apoE4-259	5	14 ± 1.9	2328 ± 105
apoE4-229	5	19 ± 4.3	2088 ± 69
apoE4-202	5	13 ± 3.4	2075 ± 78
apoE4-165	3	13 ± 4.4	1884 ± 254

(apoE2[C112/C158], apoE3[C112/R158], and apoE4[R112/R158]) as well as an apoE4 mutant where we have altered residue 158 (apoE4R158M) and several truncated apoE4 forms. These truncations produced the amino terminal segments of apoE, which extend from residue 1 to residues 259, 229, 202, or 165 of the protein. As shown in Figure 6A–H and Table 2, the binding parameters of POPC–apoE particles to apoER2 are similar for the WT apoE3 and apoE4 isoforms, the apoE4R158M mutant, and the truncated apoE forms (range of K_d 13–19 $\mu\text{g/mL}$). ApoE2 binds with slightly decreased affinity at K_d $31 \pm 5.3 \mu\text{g/mL}$. The finding suggests that the amino terminal section 1–165 of apoE contains the necessary determinants for its recognition by apoER2 and that R158M substitution has no effect on receptor binding. Previous studies have shown that binding of apoE to another apoE-recognizing receptor, the LDL receptor, requires the 171–183 region and is affected by mutations in residue 158 as well as by substitutions of charged residues in the 140–150 region of apoE (55–57).

Lipid and Lipoprotein Binding Properties of WT and Variant ApoE Forms: Implications for the Formation and the Functions of Brain Lipoproteins. Previous studies have also indicated that the region of apoE between residues 244–299, which includes half of the carboxy terminal helix 7 and the last two 11 residue long carboxy terminal helices 8 and 9 (73), contributes to the binding of apoE to lipids and lipoproteins, whereas the amino terminal region of apoE lacks the determinants required for association with lipoproteins.

In the current study, we assessed the domains of apoE involved in phospholipid binding based on the kinetics of lysis of multilamellar DMPC vesicles by the WT and variant apoE isoforms. The property of apoE to associate with phospholipids may be relevant to the biogenesis and the functions of apoE-containing lipoproteins. It was found that all of the full-length apoE forms (apoE2, apoE3, apoE4R158) solubilized multilamellar DMPC vesicles with similar kinetics. Deletion of residues 260–299 diminished greatly the ability of the truncated apoE to solubilize multilamellar DMPC vesicles and deletion of residues 230–299 or 203–299 and 166–299 eliminated completely the ability of apoE to lyse multilamellar DMPC vesicles. We have also used density gradient ultracentrifugation of culture medium of C127 cell lines expressing WT and truncated apoE2 forms to assess the effects of apoE truncations on the ability of apoE to associate with plasma lipoproteins. This analysis showed that when ^{35}S -labeled apoE was mixed with a mixture of VLDL, LDL, and HDL (d 1.006–1.18 g/mL) and then subjected to density gradient ultracentrifugation, a fraction of ^{35}S -labeled apoE was found associated with

lipoproteins in the density range of 1.006–1.21 g/mL. This fraction was approximately 17% for apoE2 and 19–21% for the truncated apoE2 forms E2-259, E2-229, and E2-165. Under the conditions of centrifugation, 10% of the apoA-I dissociated from HDL and was recovered in the $d > 1.21$ g/mL fraction. Control experiments showed that when the ultracentrifugation was performed without addition of lipoproteins in the culture medium, 97–99% of apoE secreted by these cells was found in the lipid-poor/lipid-free fraction of $d > 1.21$ g/mL (data not shown). These findings indicate that truncated apoE forms lacking the carboxy terminal residues 166–299 maintain their ability to associate with preexisting lipoproteins as the full-length forms. Taken together with our current understanding of the lipoprotein pathways, our findings indicate that the carboxy terminal 260–299 amino acids of apoE may be involved in the initial association of apoE with phospholipid, a process that may be required for the formation of apoE-containing lipoproteins. As discussed later, once apoE is lipoprotein-bound, it may be taken up by the LDL receptor and other apoE-recognizing receptors (59).

ApoE has remarkable structural similarities with apoA-I. Both proteins contain 11 or 22 amino acid long repeats, which are organized in amphipathic α -helices (73). ApoE is found in the cerebro spinal fluid associated with discoidal as well as in spherical HDL particles (62, 63); however, little is known on how these particles are formed and how they function in the brain.

Figure 7 outlines potential functions of apoE in the brain that are deduced from this study and previous papers and depicts the potential contribution of lipid-free and lipoprotein-associated apoE species in the overall lipid homeostasis in the brain.

In analogy to apoA-I (45), it is possible that the domains of apoE required for efficient interaction with phospholipids and preexisting lipoproteins may be important for the functions of apoE in the brain. In this regard, recent advances in lipoprotein research indicated that the initial step in the biogenesis of HDL in the circulation is the acquisition of membrane phospholipid and cholesterol by lipid-free apoA-I, a process that is catalyzed by ABCA1 transporter (74). This process leads to the formation of pre β 1 and subsequently to discoidal HDL particles. These particles are converted to spherical particles by the action of LCAT (75). Expression of the ABCA1 transporter has been observed in neurons in the hypothalamus, thalamus, amygdala cholinergic basal forebrain and hippocampus, and in primary cultures of neurons, astrocytes, and microglia (76). Thus, it is reasonable to assume that functional interactions of apoE with the ABCA1 transporter promote efflux of phospholipids and cholesterol and may represent an important step in the biosynthesis of apoE-containing lipoproteins in the brain. In support of this putative pathway, earlier studies showed that an HDL subfraction with γ electrophoretic mobility, designated γ LpE, is present in the plasma of apoA-I deficient mice (11, 12). It was shown that γ LpE can promote efficiently the efflux of excess cholesterol from J774 mouse macrophages (12). Thus, it is possible that lipid-free apoE as well as phospholipid-rich apoE particles formed in the brain may promote cellular efflux of cholesterol in the brain, where apoE is the only apolipoprotein. This is indicated by step 3 in Figure 7. These apoE-containing lipoprotein particles may

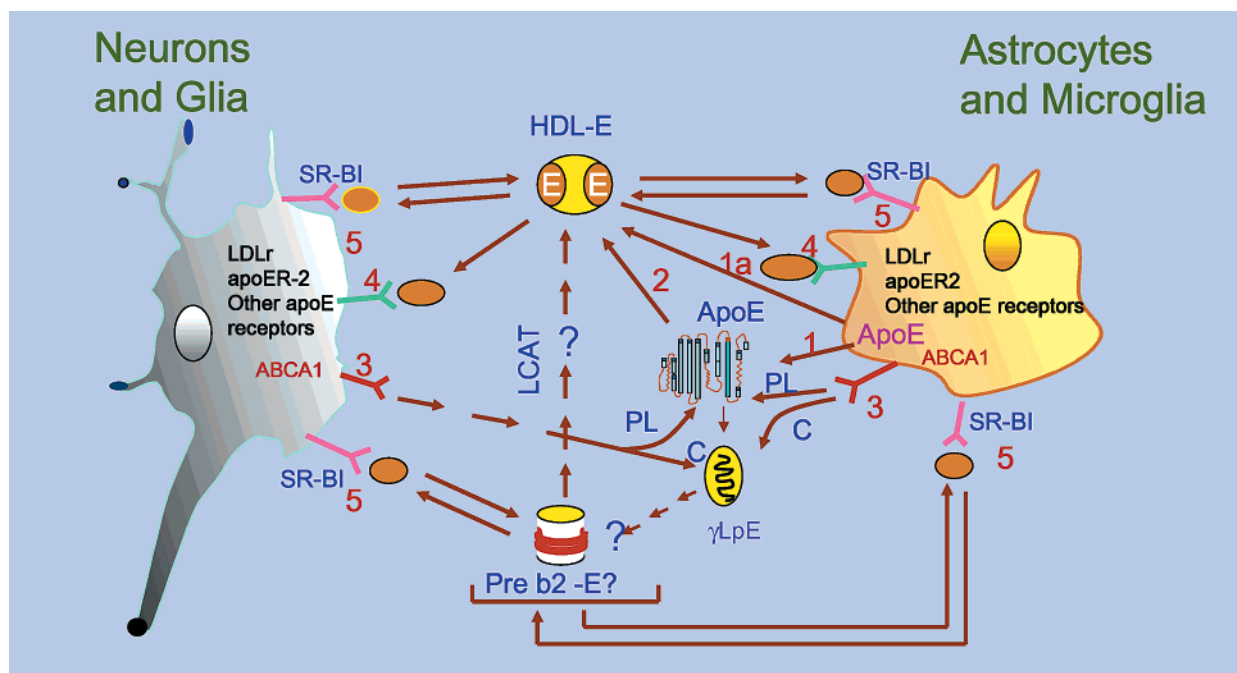


FIGURE 7: Schematic representation depicting potential contributions of apoE and apoE receptors in lipid homeostasis in the brain. Numbers 1–5 indicate different functions of apoE as follows: 1 and 2, secretion of lipid-free or lipoprotein-bound apoE by cells and incorporation of lipid-free apoE into preexisting lipoproteins; 3, formation of apoE–phospholipid complexes of γ electrophoretic mobility by the action of a lipid transporter; it is assumed that these complexes are formed by functional interactions of apoE with the ABCA1 transporter and may lead to de novo biosynthesis of apoE-containing lipoproteins in the brain (76); 4, interaction of apoE-containing lipoproteins with apoE receptors leading to unidirectional delivery of cholesterol to cells (3–7) and possibly to cell signaling (40); 5, interaction of discoidal and spherical apoE-containing lipoproteins with SR-BI leading to bidirectional exchange of cholesterol and selective uptake of lipids (77, 79, 80). The functions of apoE are inferred from the corresponding functions of this protein in the liver and the peripheral tissues. Also shown is the pathway of biosynthesis of apoE-containing lipoproteins and the role of apoE in cholesterol delivery and in cholesterol efflux.

be secreted directly by neural cells as indicated in step 1 in Figure 7 or may be formed by association of the secreted lipid-free apoE with preexisting lipoproteins as shown in steps 1 and 2 in Figure 7. Spherical HDL-E particles as well as discoidal particles, similar to the particles found in the cerebrospinal fluid, may serve to deliver unidirectionally cholesterol and other lipids to different cells via apoE-recognizing lipoprotein receptors (5, 62–64). This is indicated by step 4 in Figure 7. Finally, discoidal and spherical HDL species similar to those found in the cerebrospinal fluid may interact with SR-BI as shown in step 5 of Figure 7. This interaction will contribute to bidirectional exchange of cholesterol as well as to the selective uptake of lipids. Recent studies indicated that SR-BI is expressed by astrocytes but not by microglia in the brain (77), suggesting that interactions of apoE-containing lipoproteins with SR-BI may contribute to brain cholesterol homeostasis. We have shown recently that reconstituted POPC–apoE particles can bind to SR-BI (78) and have the ability to deliver cholesteryl esters to cells (79). The process of cholesterol efflux and cholesterol delivery is essential for cellular cholesterol homeostasis in the brain. Similar mechanisms allow cholesterol homeostasis in the liver and the peripheral tissues. The precise role of apoE-containing lipoproteins in receptor-mediated cholesterol delivery, in cholesterol efflux, and in the selective uptake of lipids in the brain, as well as the impact of the genetic variation of apoE on these processes, requires systematic in vivo and in vitro studies.

ACKNOWLEDGMENT

We thank Ms. Anne Plunkett for secretarial assistance, Ms. Angelica Chroni and Gayle Forbes for technical assistance, and Ms. Markella Zanni for editing this manuscript.

REFERENCES

- Schaefer, E. J., Gregg, R. E., Ghiselli, G., Forte, T. M., Ordovas, J. M., Zech, L. A., and Brewer, H. B., Jr. (1986) *J. Clin. Invest.* 78, 1206–1219.
- Plump, A. S., Smith, J. D., Hayek, T., Aalto-Setälä, K., Walsh, A., Verstuyft, J. G., Rubin, E. M., and Breslow, J. L. (1992) *Cell* 71, 343–353.
- Kim, D. H., Magoori, K., Inoue, T. R., Mao, C. C., Kim, H. J., Suzuki, H., Fujita, T., Endo, Y., Saeki, S., and Yamamoto, T. T. (1997) *J. Biol. Chem.* 272, 8498–8504.
- Herz, J., and Willnow, T. E. (1995) *Curr. Opin. Lipidol.* 6, 97–103.
- Wolf, M., Klug, J., Hackenberg, R., Gessler, M., Grzeschik, K. H., Beato, M., and Suske, G. (1992) *Hum. Mol. Genet.* 1, 371–378.
- Kim, D. H., Iijima, H., Goto, K., Sakai, J., Ishii, H., Kim, H. J., Suzuki, H., Kondo, H., Saeki, S., and Yamamoto, T. (1996) *J. Biol. Chem.* 271, 8373–8380.
- Takahashi, S., Kawarabayashi, Y., Nakai, T., Sakai, J., and Yamamoto, T. (1992) *Proc. Natl. Acad. Sci. U.S.A.* 89, 9252–9256.
- Wardell, M. R., Brennan, S. O., Janus, E. D., Fraser, R., and Carrell, R. W. (1987) *J. Clin. Invest.* 80, 483–490.
- Rall, S. C., Jr., Newhouse, Y. M., Clarke, H. R., Weisgraber, K. H., McCarthy, B. J., Mahley, R. W., and Bersot, T. P. (1989) *J. Clin. Invest.* 83, 1095–1101.
- Smit, M., de Knijff, P., Kooij-Meijis, E., Groenendijk, C., van den Maagdenberg, A. M., Gevers Leuven, J. A., Stalenhoef, A. F.,

- Stuyt, P. M., Frants, R. R., and Havekes, L. M. (1990) *J. Lipid Res.* 31, 45–53.
11. Huang, Y., von Eckardstein, A., Wu, S., Maeda, N., and Assmann, G. (1994) *Proc. Natl. Acad. Sci. U.S.A.* 91, 1834–1838.
 12. Huang, Y., Zhu, Y., Langer, C., Raabe, M., Wu, S., Wiesenhutter, B., Seedorf, U., Maeda, N., Assmann, G., and von Eckardstein, A. (1997) *Arterioscler., Thromb., Vasc. Biol.* 17, 2010–2019.
 13. Cullen, P., Cignarella, A., Brennhansen, B., Mohr, S., Assmann, G., and von Eckardstein, A. (1998) *J. Clin. Invest.* 101, 1670–1677.
 14. Linton, M. F., Atkinson, J. B., and Fazio, S. (1995) *Science* 267, 1034–1037.
 15. Fazio, S., Babaev, V. R., Murray, A. B., Hastly, A. H., Carter, K. J., Gleaves, L. A., Atkinson, J. B., and Linton, M. F. (1997) *Proc. Natl. Acad. Sci. U.S.A.* 94, 4647–4652.
 16. Shimano, H., Ohsuga, J., Shimada, M., Namba, Y., Gotoda, T., Harada, K., Katsuki, M., Yazaki, Y., and Yamada, N. (1995) *J. Clin. Invest.* 95, 469–476.
 17. Strittmatter, W. J., Weisgraber, K. H., Huang, D. Y., Dong, L. M., Salvesen, G. S., Pericak-Vance, M., Schmechel, D., Saunders, A. M., Goldgaber, D., and Roses, A. D. (1993) *Proc. Natl. Acad. Sci. U.S.A.* 90, 8098–8102.
 18. Corder, E. H., Saunders, A. M., Risch, N. J., Strittmatter, W. J., Schmechel, D. E., Gaskell, P. C., Jr., Rimmler, J. B., Locke, P. A., Conneally, P. M., and Schmechel, K. E. (1994) *Nat. Genet.* 7, 180–184.
 19. Corder, E. H., Saunders, A. M., Strittmatter, W. J., Schmechel, D. E., Gaskell, P. C., Small, G. W., Roses, A. D., Haines, J. L., and Pericak-Vance, M. A. (1993) *Science* 261, 921–923.
 20. Zannis, V. I., Zanni, E. E., Makrides, S. C., Kardassis, D., and Aleshkov, S. (1998) in *NATO ASI Series, Life Sciences* (Catravas, J. D., Ed.) pp 179–209, Plenum Press, New York.
 21. Boyles, J. K., Pitas, R. E., Wilson, E., Mahley, R. W., and Taylor, J. M. (1985) *J. Clin. Invest.* 76, 1501–1513.
 22. Naslund, J., Thyberg, J., Tjernberg, L. O., Wernstedt, C., Karlstrom, A. R., Bogdanovic, N., Gandy, S. E., Lannfelt, L., Terenius, L., and Nordstedt, C. (1995) *Neuron* 15, 219–228.
 23. LaDu, M. J., Falduto, M. T., Manelli, A. M., Reardon, C. A., Getz, G. S., and Frail, D. E. (1994) *J. Biol. Chem.* 269, 23403–23406.
 24. Wisniewski, T., Golabek, A., Matsubara, E., Ghiso, J., and Frangione, B. (1993) *Biochem. Biophys. Res. Commun.* 192, 359–365.
 25. Aleshkov, S., Abraham, C. R., and Zannis, V. I. (1997) *Biochemistry* 36, 10571–10580.
 26. Aleshkov, S. B., Li, X., Lavrentiadou, S. N., and Zannis, V. I. (1999) *Biochemistry* 38, 8918–8925.
 27. Strittmatter, W. J., Saunders, A. M., Goedert, M., Weisgraber, K. H., Dong, L. M., Jakes, R., Huang, D. Y., Pericak-Vance, M., Schmechel, D., and Roses, A. D. (1994) *Proc. Natl. Acad. Sci. U.S.A.* 91, 11183–11186.
 28. Barger, S. W., and Mattson, M. P. (1997) *J. Neurochem.* 69, 60–67.
 29. Poirier, J., Delisle, M. C., Quirion, R., Aubert, I., Farlow, M., Lahiri, D., Hui, S., Bertrand, P., Nalbantoglu, J., and Gilfix, B. M. (1995) *Proc. Natl. Acad. Sci. U.S.A.* 92, 12260–12264.
 30. Soininen, H., Kosunen, O., Helisalmi, S., Mannermaa, A., Paljarvi, L., Talasniemi, S., Ryyanen, M., and Riekkinen, P., Sr. (1995) *Neurosci. Lett.* 187, 79–82.
 31. Arendt, T., Schindler, C., Bruckner, M. K., Eschrich, K., Bigl, V., Zedlick, D., and Marcova, L. (1997) *J. Neurosci.* 17, 516–529.
 32. Bellosa, S., Nathan, B. P., Orth, M., Dong, L. M., Mahley, R. W., and Pitas, R. E. (1995) *J. Biol. Chem.* 270, 27063–27071.
 33. Buttini, M., Orth, M., Bellosa, S., Akeefe, H., Pitas, R. E., Wyss-Coray, T., Mucke, L., and Mahley, R. W. (1999) *J. Neurosci.* 19, 4867–4880.
 34. Holtzman, D. M., Bales, K. R., Tenkova, T., Fagan, A. M., Parsadanian, M., Sartorius, L. J., Mackey, B., Olney, J., McKeel, D., Wozniak, D., and Paul, S. M. (2000) *Proc. Natl. Acad. Sci. U.S.A.* 97, 2892–2897.
 35. Holtzman, D. M., Bales, K. R., Wu, S., Bhat, P., Parsadanian, M., Fagan, A. M., Chang, L. K., Sun, Y., and Paul, S. M. (1999) *J. Clin. Invest.* 103, R15–R21.
 36. Bales, K. R., Verina, T., Cummins, D. J., Du, Y., Dodel, R. C., Saura, J., Fishman, C. E., DeLong, C. A., Piccardo, P., Petegnief, V., Ghetti, B., and Paul, S. M. (1999) *Proc. Natl. Acad. Sci. U.S.A.* 96, 15233–15238.
 37. Esser, V., Limbird, L. E., Brown, M. S., Goldstein, J. L., and Russell, D. W. (1988) *J. Biol. Chem.* 263, 13282–13290.
 38. Herz, J., and Beffert, U. (2000) *Nat. Rev. Neurosci.* 1, 51–58.
 39. Hiesberger, T., Trommsdorff, M., Howell, B. W., Goffinet, A., Mumbly, M. C., Cooper, J. A., and Herz, J. (1999) *Neuron* 24, 481–489.
 40. Trommsdorff, M., Gotthardt, M., Hiesberger, T., Shelton, J., Stockinger, W., Nimpf, J., Hammer, R. E., Richardson, J. A., and Herz, J. (1999) *Cell* 97, 689–701.
 41. Liadaki, K. N., Liu, T., Xu, S., Ishida, B. Y., Duchateaux, P. N., Krieger, J. P., Kane, J., Krieger, M., and Zannis, V. I. (2000) *J. Biol. Chem.* 275, 21262–21271.
 42. He, T. C., Zhou, S., da Costa, L. T., Yu, J., Kinzler, K. W., and Vogelstein, B. (1998) *Proc. Natl. Acad. Sci. U.S.A.* 95, 2509–2514.
 43. Fallaux, F. J., Kranenburg, O., Cramer, S. J., Houweling, A., Van Ormondt, H., Hoebe, R. C., and van der Eb, A. J. (1996) *Hum. Gene Ther.* 7, 215–222.
 44. Cladaras, C., Hadzopoulou-Cladaras, M., Felber, B. K., Pavlakis, G., and Zannis, V. I. (1987) *J. Biol. Chem.* 262, 2310–2315.
 45. Laccotripe, M., Makrides, S. C., Jonas, A., and Zannis, V. I. (1997) *J. Biol. Chem.* 272, 17511–17522.
 46. Pownall, H. J., Massey, J. B., Kusserow, S. K., and Gotto, A. M., Jr. (1978) *Biochemistry* 17, 1183–1188.
 47. Matz, C. E., and Jonas, A. (1982) *J. Biol. Chem.* 257, 4535–4540.
 48. Markwell, M. A. (1982) *Anal. Biochem.* 125, 427–432.
 49. Brenner, A. J., and Harris, E. D. (1995) *Anal. Biochem.* 226, 80–84.
 50. Krieger, M. (1983) *Cell* 33, 413–422.
 51. Sege, R. D., Kozarsky, K. F., and Krieger, M. (1986) *Mol. Cell Biol.* 6, 3268–3277.
 52. Gu, X., Trigatti, B., Xu, S., Acton, S., Babbitt, J., and Krieger, M. (1998) *J. Biol. Chem.* 273, 26338–26348.
 53. Zanni, E. E., Kouvatzi, A., Hadzopoulou-Cladaras, M., Krieger, M., and Zannis, V. I. (1989) *J. Biol. Chem.* 264, 9137–9140.
 54. Wernette-Hammond, M. E., Lauer, S. J., Corsini, A., Walker, D., Taylor, J. M., and Rall, S. C., Jr. (1989) *J. Biol. Chem.* 264, 9094–9101.
 55. Rall, S. C., Jr., Weisgraber, K. H., Innerarity, T. L., and Mahley, R. W. (1982) *Proc. Natl. Acad. Sci. U.S.A.* 79, 4696–4700.
 56. Lalazar, A., Weisgraber, K. H., Rall, S. C., Jr., Giladi, H., Innerarity, T. L., Levanon, A. Z., Boyles, J. K., Amit, B., Gorecki, M., and Mahley, R. W. (1988) *J. Biol. Chem.* 263, 3542–3545.
 57. Lalazar, A., and Mahley, R. W. (1989) *J. Biol. Chem.* 264, 8447–8450.
 58. van Vlijmen, B. J., Van Dijk, K. W., van't Hof, H. B., van Gorp, P. J., van Der, Z. A., van der, B. H., Breuer, M. L., Hofker, M. H., and Havekes, L. M. (1996) *J. Biol. Chem.* 271, 30595–30602.
 59. Kypreos, K. E., Morani, P., Van Dijk, K. W., Havekes, L. M., and Zannis, V. I. (2001) *Biochemistry* 40, 6027–6035.
 60. Kypreos, K. E., Teusink, B., Van Dijk, K. W., Havekes, L. M., and Zannis, V. I. (2001) *FASEB J.* 15, 1598–1600.
 61. Ji, Z. S., Fazio, S., Lee, Y. L., and Mahley, R. W. (1994) *J. Biol. Chem.* 269, 2764–2772.
 62. Borghini, I., Barja, F., Pometta, D., and James, R. W. (1995) *Biochim. Biophys. Acta* 1255, 192–200.
 63. Pitas, R. E., Boyles, J. K., Lee, S. H., Hui, D., and Weisgraber, K. H. (1987) *J. Biol. Chem.* 262, 14352–14360.
 64. Swanson, L. W., Simmons, D. M., Hofmann, S. L., Goldstein, J. L., and Brown, M. S. (1988) *Proc. Natl. Acad. Sci. U.S.A.* 85, 9821–9825.
 65. Christie, R. H., Chung, H., Rebeck, G. W., Strickland, D., and Hyman, B. T. (1996) *J. Neuropathol. Exp. Neurol.* 55, 491–498.
 66. Innerarity, T. L., Friedlander, E. J., Rall, S. C., Jr., Weisgraber, K. H., and Mahley, R. W. (1983) *J. Biol. Chem.* 258, 12341–12347.
 67. Weisgraber, K. H., Innerarity, T. L., Harder, K. J., Mahley, R. W., Milne, R. W., Marcel, Y. L., and Sparrow, J. T. (1983) *J. Biol. Chem.* 258, 12348–12354.
 68. Weisgraber, K. H., Rall, S. C., Jr., Mahley, R. W., Milne, R. W., Marcel, Y. L., and Sparrow, J. T. (1986) *J. Biol. Chem.* 261, 2068–2076.
 69. Weisgraber, K. H. (1990) *J. Lipid Res.* 31, 1503–1511.
 70. Dong, L. M., and Weisgraber, K. H. (1996) *J. Biol. Chem.* 271, 19053–19057.
 71. Westerlund, J. A., and Weisgraber, K. H. (1993) *J. Biol. Chem.* 268, 15745–15750.
 72. Dong, L. M., Wilson, C., Wardell, M. R., Simmons, T., Mahley, R. W., Weisgraber, K. H., and Agard, D. A. (1994) *J. Biol. Chem.* 269, 22358–22365.

73. Nolte, R. T., and Atkinson, D. (1992) *Biophys. J.* 63, 1221–1239.
74. Schmitz, G., and Langmann, T. (2001) *Curr. Opin. Lipidol.* 12, 129–140.
75. Warden, C. H., Langner, C. A., Gordon, J. I., Taylor, B. A., McLean, J. W., and Lusi, A. J. (1989) *J. Biol. Chem.* 264, 21573–21581.
76. Koldamova, R. P., Lefterov, I. M., Ikonovic, M. D., Skoko, J., Lefterov, P. I., Isanski, B. A., DeKosky, S. T., and Lazo, J. S. (2003) *J. Biol. Chem.* 278, 13244–13256.
77. Husemann, J., and Silverstein, S. C. (2001) *Am. J. Pathol.* 158, 825–832.
78. Li, X., Kan, H. Y., Lavrentiadou, S., Krieger, M., and Zannis, V. (2002) *J. Biol. Chem.* 277, 21149–21157.
79. Thuahnai, S. T., Lund-Katz, S., Williams, D. L., and Phillips, M. C. (2001) *J. Biol. Chem.* 276, 43801–43808.
80. Krieger, M. (2001) *J. Clin. Invest.* 108, 793–797.

BI027093C